

TOWARDS A STRUCTURAL VIEW OF GATING IN POTASSIUM CHANNELS

Kenton J. Swartz

Abstract | Voltage-activated cation channels have pores that are selective for K^+ , Na^+ or Ca^{2+} . Neurons use these channels to generate and propagate action potentials, release neurotransmitters at synaptic terminals and integrate incoming signals in dendrites. Recent X-ray and electron microscopy studies of an archaeobacterial voltage-activated K^+ (Kv) channel have provided the first atomic resolution images of the voltage-sensing domains in Kv channels. Although these structures are consistent with previous biophysical analyses of eukaryotic channels, they also contain surprises, which have provoked new ideas about the structure and movements of these proteins during gating. This review summarizes our current understanding of these intriguing membrane proteins and highlights the open questions.

MEMBRANE CONDUCTANCE

The movement of charged ions across biological membranes gives rise to an electrical current. Conductance is a measure of how readily these currents flow across the membrane.

Molecular Physiology and Biophysics Section, Porter Neuroscience Research Center, National Institute of Neurological Disorders and Stroke, National Institutes of Health, 35 Convent Drive, MSC 3701, Bethesda, Maryland 20892-3701. e-mail: swartzk@ninds.nih.gov doi:10.1038/nrn1559

Excitable cells use a bewildering array of membrane proteins to generate electrical and chemical signals. In the early 1950s, Hodgkin and Huxley established the presence of MEMBRANE CONDUCTANCES for K^+ and Na^+ that underlie the action potential in the squid giant axon¹⁻⁴, commencing the past half-century of investigation into the physical mechanisms underlying these conductances. Interestingly, these ion conductances switch on and off with changes in membrane voltage. It is now appreciated that these gated conductances arise from a family of membrane proteins that have three crucial functional elements: an ion conduction pore that can distinguish between K^+ , Na^+ and Ca^{2+} ; a gate that minimizes the flow of ions in the closed state; and voltage sensors that detect changes in membrane voltage and trigger opening and closing of the gate. For the classical voltage-activated channels that were studied by Hodgkin and Huxley, the probability that the gate is open is low at HYPERPOLARIZED membrane voltages, but increases significantly in response to membrane DEPolarization. Contemporary experiments on the Shaker Kv channel, a particularly well-studied voltage-activated channel from *Drosophila melanogaster*^{5,6}, show that the open probability varies over a broad range, from values of perhaps 10^{-9} at negative voltages to positive voltages of close to 1 (REFS 7-14), indicating that these channels can respond to changes in membrane voltage with extraordinarily high

precision. This review focuses on the mechanisms that underlie voltage-dependent activation in Kv channels, with occasional reference to their Na^+ - or Ca^{2+} -selective counterparts (Nav or Cav channels, respectively). The recent success in solving the atomic resolution structures of prokaryotic K^+ (REFS 15-20) and Cl⁻ channels²¹, when combined with the recent identification of prokaryotic Na^+ channels^{22,23}, provides grounds for optimism about unravelling the structures of other types of voltage-activated cation channel.

Architecture of Kv channels

Kv channels belong to a diverse family of cation channels that includes Nav and Cav channels²⁴⁻²⁶, cyclic nucleotide-activated channels²⁷, hyperpolarization-activated cation channels²⁸, Ca^{2+} -activated K^+ channels²⁹, inward rectifier K^+ channels³⁰⁻³², two-pore K^+ channels^{33,34} and glutamate-activated channels³⁵ (FIG. 1). The functional Kv channel is a tetramer^{36,37} with four identical (or similar) subunits. The conventional topology of the S1 to S6 transmembrane segments in each subunit is based on evidence for positioning specific regions on either the intracellular or extracellular side of the membrane (FIG. 1). For example, the region on the amino (N)-terminal side of S1 in the Shaker Kv channel is thought to function as a tethered intracellular blocker of the pore^{17,38,39}, which underlies fast inactivation and

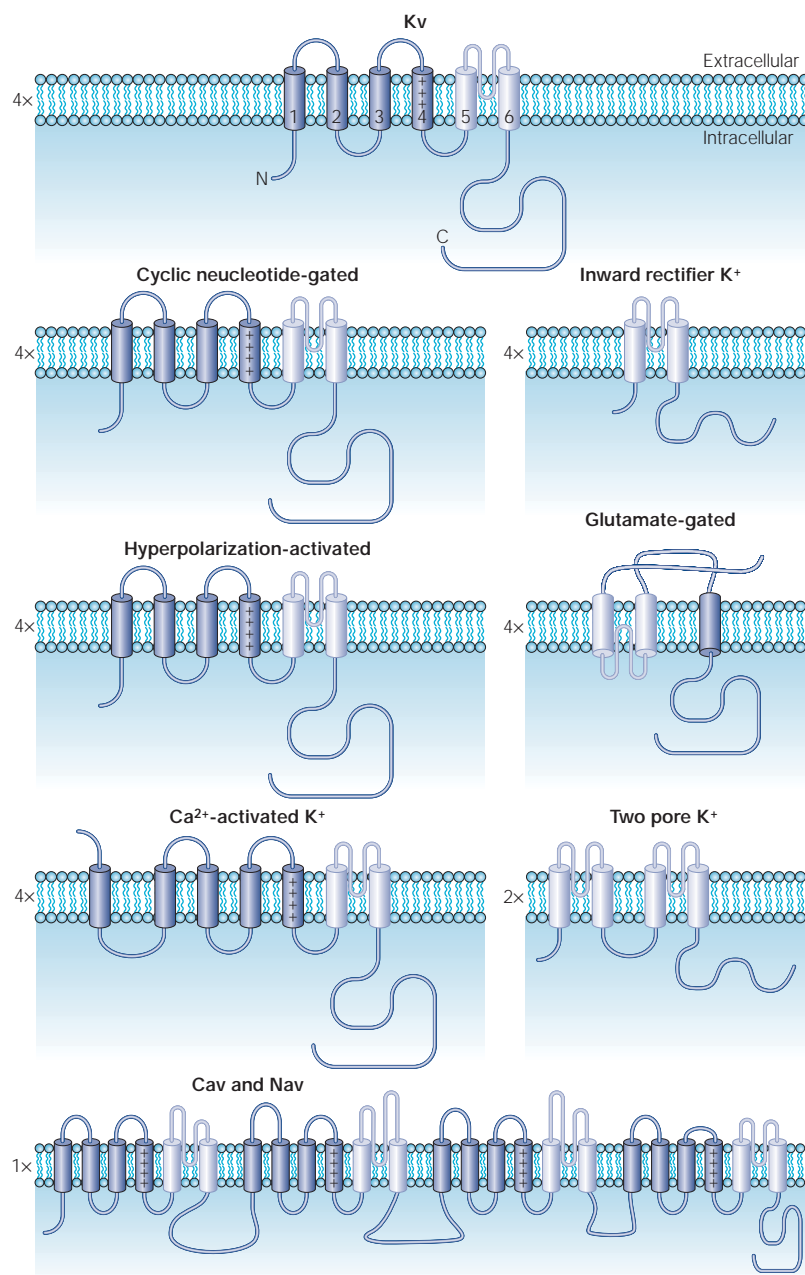


Figure 1 | **Membrane folding model for Kv and related cation channels.** The models are oriented with their extracellular sides up. The light blue transmembrane regions form the ion conduction pores in a tetrameric arrangement.

**HYPERPOLARIZATION/
DEPOLARIZATION**

In most electrically polarized cell membranes the intracellular side is more negatively charged relative to the extracellular side, and the voltage across the membrane is said to be negative. Depolarization signifies a change in membrane voltage whereby the inside becomes more positive; hyperpolarization a change whereby the inside becomes more negative.

indicates that the N terminus is intracellular. The linker between S1 and S2 is glycosylated⁴⁰ and must, therefore, be extracellular. A native cysteine residue between S2 and S3 can be modified by internally applied methanethio-sulphonate (MTS) reagents⁴¹, which indicates an intracellular location. Studies on protein toxins that bind to the carboxy (C) terminus of S3 in the Kv2.1 channel indicate that this region of the channel is near the extracellular solution^{42–44}. Finally, the N terminus of S4 is accessible to extracellular MTS reagents, whereas both the C terminus of S4 and the S4–S5 linker are accessible to these reagents when they are applied to the intracellular

side^{41,45–47}. The topology and structure of the S5–S6 region is the best defined because it is well conserved across K⁺ channels, and four K⁺ channel structures have now been solved^{15,18–20}.

The gate region in K⁺ channels

The gate region in K⁺ channels controls whether ions can traverse the ion conduction pore. In Kv channels, the pore domain is formed by S5 through S6, with S6 and the S5–S6 linker lining the ion conduction pathway. Initial support for this model was provided by studies with pore-blocking toxins that bind to the extracellular region between S5 and S6^{48,49}. More recently, the X-RAY STRUCTURE of the KcsA K⁺ channel^{15,16} (FIG. 2a) — a relatively simple prokaryotic channel with two transmembrane segments that are similar to S5 and S6 in Kv channels — established the pore-forming nature of this region and showed how K⁺ ions are coordinated by backbone carbonyl atoms near the extracellular end of the pore. Although the pathway that K⁺ ions use to cross the membrane is now clear, how the flow of ions is regulated is less well understood. In the late 1960s, Armstrong found that quaternary ammonium (QA) compounds could block the squid giant axon Kv channel when applied from the intracellular side of the membrane, but only after the gate had been opened by membrane depolarization^{50–52}. In addition, if the gate is rapidly closed by strong hyperpolarization of the membrane, QA blockers can be trapped in the channel. Armstrong proposed that a gate was located on the intracellular side of the membrane and that there must be a cavity on the extracellular side of the gate in which QAs could reside⁵².

In the Shaker Kv channel, the intracellular gate cannot close when QAs are bound within the pore unless a point mutation in the S6 transmembrane segment is introduced that converts the isoleucine residue at position 470 to Cys⁵³. This bolsters Armstrong's interpretation and further implicates the intracellular region of S6 in forming the gate. Moreover, the reactions between water-soluble MTS reagents and Cys residues show a region in the intracellular end of S6 where reaction rates abruptly change from having little state dependence to having a striking (up to 10⁵-fold) preference for the open state⁵⁴. Similar experiments have also shown gated access of Ag⁺, a small thiol-reactive ion with dimensions and diffusion properties similar to K⁺ (REF. 55). A Cd²⁺ bridge between Cys and histidine residues in intracellular regions of adjacent S6 segments can lock the gate open⁵⁶, and mutations in the intracellular end of S6 can cause either constitutive activation⁵⁷ or prevent the gate from opening⁵⁸. Taken together, these data are consistent with the location of a gate at the intracellular entrance to the ion conduction pore in Kv channels.

The X-ray structure of the KcsA K⁺ channel shows that the helices of the second transmembrane segment (corresponding to S6 in Kv channels) adopt an inverted teepee-like architecture at the intracellular end of the pore, which leaves a large aqueous cavity that could accommodate QA blockers just above a bundle crossing that seems to be in a closed conformation^{15,59} (FIG. 2).

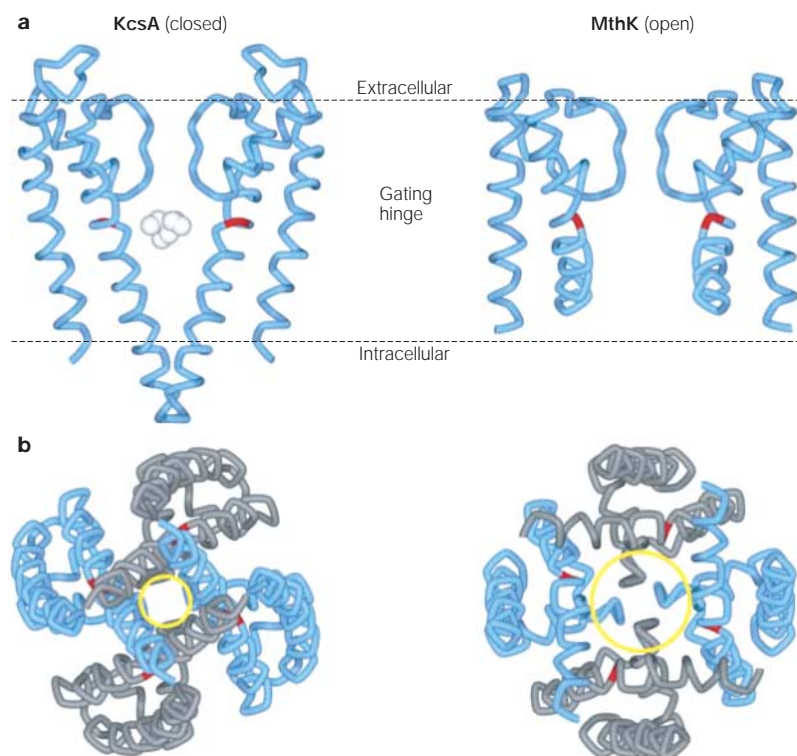


Figure 2 | X-ray structures of KcsA and MthK potassium channels. **a** | Side view of the two channels with the front and back subunits removed for clarity. The red residue in both channels (G99 in KcsA and G83 in MthK) is a glycine residue that has been proposed to serve as a gating hinge. The white molecule in the cavity of KcsA (closed) is a quaternary ammonium blocker. **b** | View of the tetrameric channels from an intracellular vantage point. The difference in aperture of the intracellular entrance to the pore in the two channels is outlined with a yellow ring. Protein database accession codes are 1J95 for KcsA and 1LNQ for MthK. Structures were generated using DS Viewer Pro (Accelrys).

The structure of a KcsA–QA complex showed that QAs (the white molecule in FIG. 2a) bind in the cavity¹⁷. The structure of the MthK channel, a prokaryotic Ca^{2+} -activated K^+ channel, refined the picture of the gate further because this channel was caught in what appears to be an open state^{18,60} (FIG. 2). The aperture of the internal pore (~12 Å) in the open MthK structure is much larger than that of the KcsA structure, which is consistent with the idea that gating involves changes in the dimensions of the internal pore, from a KcsA-like structure when closed to an MthK-like structure when open. In this view, the second transmembrane segment helices would undergo a large splaying motion at the position of a conserved glycine residue above the occluding region⁶⁰ (red residue in FIG. 2). These structural features, combined with ELECTRON PARAMAGNETIC RESONANCE (EPR)^{61,62}, accessibility⁶³ and mutagenesis⁶⁴ studies of KcsA and the data from Kv channels, all support the presence of a gate at the intracellular bundle crossing.

Diversity in gate structure and motions
Although there is strong support for a gate at the intracellular side of the pore in K^+ channels, there is mounting evidence for variations in the structure of the gate region and in the movements that occur during opening. First, the intracellular end of S6 in many Kv channels

(for example, Shaker) has a unique proline–valine–proline (PVP) motif that is absent from KcsA and MthK. The propensity of Pro to bend or kink helices⁶⁵ indicates that this region of Shaker might adopt a different structure. Second, the pattern of blocker-mediated protection of introduced Cys residues from reactions with MTS reagents⁶⁶, as well as the accessibility of large MTS reagents⁶⁵, point to an abrupt enlargement of the pore just below the PVP motif, which is consistent with a bent S6 helix (FIG. 3). Third, an inter-subunit METAL BRIDGE between a mutated residue, V476C, and His at position 486 in Shaker locks the channel in an open conformation (FIG. 3), but the corresponding residues are too far apart to coordinate metals in the structure of either the closed KcsA channel or the open MthK channel^{56,66,67}. These discrepancies support a bent S6 model for the intracellular gate region in the Shaker Kv channel⁶⁷ (FIG. 3), indicating that the structure of the gate in Kv channels is significantly different from the observed X-ray structures of KcsA and MthK (FIG. 2).

The coordination of Cd^{2+} by Cys residues substituted for Val in the PVP motif of Shaker raises the possibility that the motions of the gate in this Kv channel also differ from suggestions made from comparisons between KcsA and MthK. Yellen and colleagues have shown that a Cd^{2+} ion can be simultaneously coordinated by at least three Cys residues substituted at V474 (FIG. 3), a region that corresponds to the bundle crossing in KcsA⁶⁴. When the voltage-dependence of Cd^{2+} release from V474C is investigated using dimercaptopropane-sulphonate (DMPS) — a di-thiol compound that displaces the thiol groups of the protein involved in coordinating Cd^{2+} — the voltage-dependence of release parallels the voltage-dependence of channel opening^{54,67}. Although this result indicates that a gate below residue 474 regulates the access of DMPS, it also implies that the open–closed equilibrium is not significantly altered when Cd^{2+} is bound at 474. This, combined with other evidence against bridge-induced distortions of gate structure⁶⁷, indicates that V474 moves little between the open and closed states, which is inconsistent with the idea that the gate moves between a KcsA-like structure when closed and an MthK-like structure when open. These studies indicate that the structure and motions of the gate region in Kv channels might differ substantially from that proposed for KcsA and MthK⁶⁰.

The voltage-sensors in the Kv channels
Hodgkin and Huxley were first to suggest that the voltage sensitivity of the K^+ and Na^+ conductances in the squid giant axon arises from the movement of charged particles within the membrane electric field⁴. That there are charge movements associated with the voltage-sensitivity of voltage-activated ion channels was subsequently shown by Armstrong and Bezanilla^{68,69} and Keynes and Rojas⁷⁰ working on the squid giant axon, and by Schneider and Chandler^{71,72} working on skeletal muscle. Under conditions where voltage-activated channels are present at high density and ion conduction has been effectively eliminated, depolarization of the membrane elicits a transient outward current (upward current

X-RAY STRUCTURE

In X-ray crystallography of proteins, a crystallized protein is bombarded with X-rays and the diffraction pattern is used to develop a three dimensional model of the protein's atomic structure. This model is often termed the X-ray structure of the protein.

ELECTRON PARAMAGNETIC RESONANCE

(EPR). A spectroscopic technique based on the magnetic moment of an unpaired free electron. Although proteins typically have little EPR signal, spin-labels with unpaired electrons can be attached to the protein and EPR used to provide information about the mobility and solvent accessibility of the spin-label. EPR can also be used to obtain distances between spin labels and another paramagnetic atom.

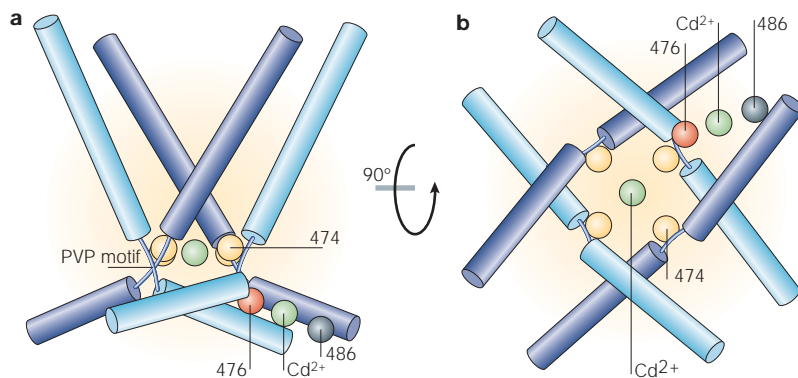


Figure 3 | Illustration of the bent S6 model in an open Kv channel and two types of Cd²⁺ bridges. **a** | Side view of the S6 (transmembrane subunit) helices, corresponding to the second transmembrane segment inner helices (S2) in KcsA or MthK. In the first type of bridge, Cd²⁺ (light green) bridges cysteine at position 476 (red) and histidine at 486 (dark green) between adjacent subunits (only one of four possible bridges is shown), which locks the channel open. In the second type, at least three Cys residues introduced at valine 474 coordinate Cd²⁺ at the central axis of the pore. **b** | Intracellular view of the bent S6 helices and the two bridges.

deflection) that corresponds to the movement of positive charge from inside to outside, known as an On gating current⁷³ (FIG. 4a). After subsequent repolarization, a transient inward current (downward current deflection), known as the Off gating current, is observed. The integrals of both On- and Off-current components

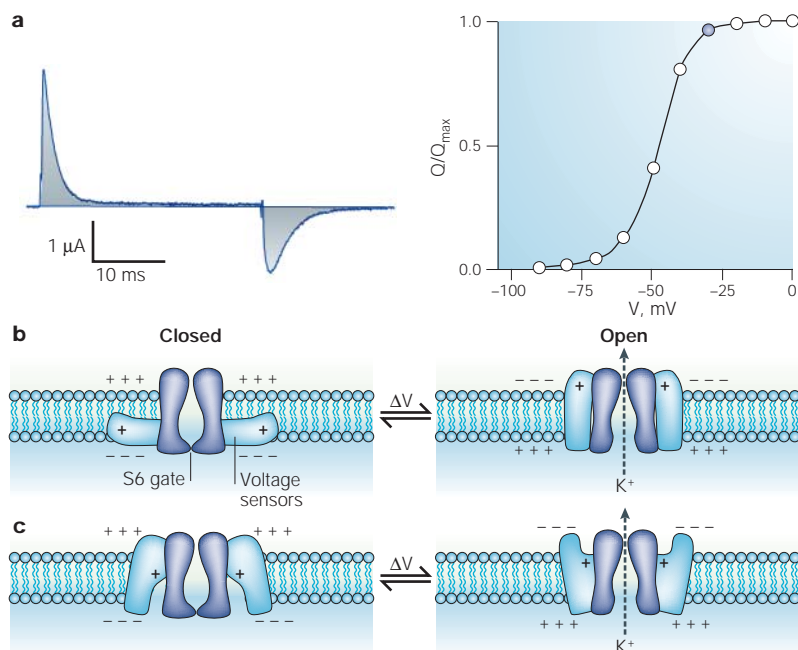


Figure 4 | Charge movement in Kv channels. **a** | Gating currents recorded from a cell expressing the Shaker Kv channel. The membrane voltage was initially held at -90 mV and the On gating current (upward deflection) was elicited by depolarizing to a test voltage of -30 mV. The Off gating current (downward deflection) was elicited by repolarization from -30 mV back to the holding voltage of -90 mV. The area under the current trace (grey shading) corresponds to the amount of charge moved. A 'P/-4' protocol⁷³ was used to subtract leak and linear capacitive currents and a phenylalanine substitution for tryptophan at position 434 (REF 142) was introduced to make the channel nonconducting. The graph on the right shows the relationship between normalized charge (Q/Q_{max}) and test voltage (V). **b** | Schematic diagram of the membrane translocation model for charge movement, where charges in the voltage-sensor move from one side of the membrane to the other. **c** | Schematic diagram of the focused field model, in which charges move a short distance between water-filled crevices in the protein that serve to focus the membrane electric field.

(grey shading in FIG. 4a) are equal to the quantity of charge (Q) that has moved; they have the same values but opposite signs because they correspond to the movement of the same charges from a resting to an activated position and back. The energetics of charge movement can be described by plotting Q as a function of voltage (FIG. 4a), which shows the saturation of charge movement and its association with movements of the protein between distinct conformations. How much charge is translocated when a voltage-activated channel is activated? In the case of the Shaker Kv channel, direct measurements indicate that the equivalent of between 12 and 14 electronic charges move across the entire membrane electric field when a single channel is activated⁷⁴⁻⁷⁷, or about 3 to 3.5 charges per subunit. Similar estimates of charge per channel have been obtained for Cav (REF. 77) and Nav (REF. 78) channels.

Which region of the protein detects the changes in membrane voltage and what is the structural basis of the underlying charge movement? When the first voltage-activated channels were cloned, the S4 segment, which is rich in positively charged basic residues, was recognized as a potential voltage-sensor^{5,6,24-26}. Mutations that neutralize the charges of these residues in S4 alter both the voltage-activation⁷⁹⁻⁸⁴ and the relationship between gating charge and voltage⁸⁵, and decrease the amount of charge that is moved on activation of the channel^{75,76,86}. Movements of S4 from internal to external have been inferred from the state-dependence of MTS reactivity with Cys residues that are substituted at a number of positions in this segment^{45-47,87} and from proton transport by introduced His residues^{88,89}. In addition, fluorescent probes attached near S4 show voltage-dependent changes in FLUORESCENCE that have the time and voltage-dependence expected of the voltage-sensor⁹⁰⁻⁹⁵. These results indicate that S4 is important in voltage sensing. Mutations of negatively charged acidic residues in S2 and S3 also perturb the voltage-activation relationship, the voltage-dependence of gating currents and the amount of charge translocated per channel, which is consistent with a role for these segments in voltage-sensing^{76,96-98}.

Conceptual views of voltage-sensing

Although it is agreed that S4 is involved in voltage-sensing, the conceptual and structural basis for gating charge movement is the subject of intense controversy. The debate can be captured by considering two models for the movement of gating charge. The 'membrane translocation model' proposes that the gating charges completely translocate from one side of the hydrophobic phase of the membrane to the other, which corresponds to a movement of more than 20 Å (FIG. 4b). In the simplest form of this model, the gating charges in the protein can be regarded as tethered hydrophobic cations that move through the hydrophobic phase of the membrane. By contrast, the 'focused field model' proposes that charges move shorter distances between water-filled crevices in the protein that serve to focus the electric field of the membrane (FIG. 4c). An important distinction is that the charges directly sense the voltage drop across the lipid membrane in the membrane translocation model,

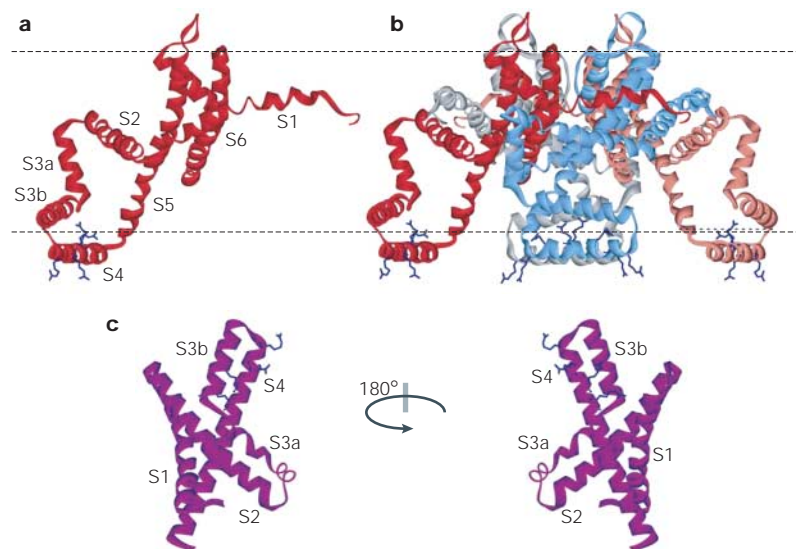


Figure 5 | X-ray structures of the KvAP channel and the isolated S1–S4 domain. Ribbon diagrams for the structure of a single subunit (**a**) and tetrameric (**b**) KvAP channel, or the isolated S1–S4 domain (**c**). The structures that comprise the intact KvAP channel are oriented with the extracellular side of the protein facing up. Dashed lines demarcate the approximate boundaries of the membrane. Protein database accession codes are 1ORQ for the intact channel structures in **a** and **b**, and 1ORS for the isolated S1–S4 domain in **c**. Structures were generated using DS Viewer Pro (Accelrys).

whereas the charges sense the voltage drop across the protein in the focused field model. Although these models are conceptual, they incite different structural expectations. For example, the membrane translocation model would be in line with an X-ray structure where important parts of the voltage-sensor are on one side of the membrane or the other. (Recall that the protein must adopt a particular uniform conformation for ordered crystals to be grown and its structure solved by X-ray crystallography.) Conversely, the focused field model conjures up images of a structure where important parts of the voltage-sensor take on a transmembrane orientation, with water-filled crevices projecting from aqueous phases. In addition, S4 might be shrouded by the S1–S3 transmembrane segments, thereby protecting the charges from the bilayer and providing a convenient way of constructing crevices. Although a number of distinct theories of voltage-sensing have been proposed, most are closely aligned with the focused field model^{45,46,76,86,88,89,94,96,99–110}. In the late spring of 2003 the X-ray structure of the KvAP channel was reported²⁰ and the pot was given a brisk stir.

X-ray structure of the KvAP channel
The KvAP channel is a prokaryotic K⁺-selective channel from the hyperthermophilic archaeobacterium *Aeropyrum pernix*¹¹¹. When incorporated into lipid bilayers, KvAP supports voltage-activated K⁺ currents with a voltage-activation relationship similar to that of the Shaker Kv channel¹¹¹. KvAP is inhibited by charybdotoxin¹¹¹, a classical pore-blocking toxin that recognizes the external entrance to the ion conduction pore in various types of K⁺ channel¹¹², and by VSTx¹¹¹, a toxin that is related to those that interact with voltage-sensors in Kv

channels^{42–44,113,114}. The X-ray structure of the intact KvAP protein was solved to 3.2 Å resolution with FAB FRAGMENTS of monoclonal antibodies bound to the voltage-sensors²⁰; these have been removed for clarity from the ribbon diagrams in FIG. 5. The pore forming region of KvAP consists of the S5 and S6 transmembrane helices, with a short pore helix and selectivity filter in the S5–S6 linker, which is consistent with the structures of KcsA, MthK and K_vBac. The SECONDARY STRUCTURE of the voltage-sensing domain in S1–S4 is also consistent with previous studies^{43,99,115,116}, as illustrated by a comparison between the α -helical periodicity profile obtained from scanning mutagenesis in Kv2.1 and the position of helices within the X-ray structures of KvAP (FIG. 6b). The unexpected aspects of the KvAP X-ray structure concern the TERTIARY STRUCTURE of the S1–S4 domain. Instead of adopting a transmembrane orientation, S4 lies parallel to the intracellular side of the membrane plane; S1 and S2 meander through the depths of the membrane; and only the S4 and S3b helices are tightly packed, forming a helix–turn–helix motif known as the voltage-sensor paddle. On first sight, if you are in the membrane translocation camp you can't help but like the structure, but if you are in the focused field camp you are probably gasping for air! A higher resolution (1.9 Å) structure of the isolated S1–S4 domain shows similar secondary structural elements, whereas the tertiary structure is different²⁰ (FIG. 5c). There are many side chains buried in the isolated domain, which indicates more extensive packing, and the orientation of the domain relative to the membrane is unknown.

Distortions of the KvAP X-ray structure
MacKinnon and colleagues pointed out several reasons for suggesting that there could be distortions in the X-ray structure of KvAP (REF. 20). First, the position of the S6 helices in KvAP is consistent with an open conformation, but the voltage-sensor paddles are positioned towards the intracellular edge of the membrane where they might approximate a resting conformation. A comparison between this region in two closed channels, KcsA and K_vBac, and the open MthK channel (FIG. 7b) indicates that the S6 gate is open in KvAP. This apparent contradiction is a clear indication of distortion, considering how effective the voltage-sensors are at controlling the conformation of the gates in the native environment. In the Shaker Kv channel, for example, the open probability for the gate is below 10^{–9} at negative voltages where the voltage-sensors are resting¹³. To see voltage-sensors in a position that approximates a resting conformation, with a gate that is open, would be improbable if the protein were adopting a native-like structure. Second, some eukaryotic Kv channels have glycosylation sites in the S1–S2 linkers^{40,117}, which indicates that the C terminus of S1 and the N terminus of S2 should be near the extracellular surface, but in the KvAP structure these regions are buried in the middle of the membrane. Third, the pore-blocking properties of the N-terminal inactivation domain indicate that the N terminus of S1 could have a cytoplasmic location (REFS 17,38,39), but in the KvAP structure this region is in the middle of the membrane.

METAL BRIDGE

A bridge formed by the coordination of a metal ion by two or more amino acid side chains. The most common bridges use the metals Cd²⁺ and Zn²⁺, and involve coordination by cysteine and histidine residues.

FLUORESCENCE

The process by which light is emitted from a substance, typically an aromatic molecule, when an electron in an excited singlet state returns to the ground state. Fluorescence emissions tend to be sensitive to the environment surrounding the fluorophore.

FAB FRAGMENTS

Cleavage of an immunoglobulin with papain releases two Fab fragments, each capable of recognizing antigen, and a single Fc fragment. Fab fragments that recognize motifs in membrane proteins facilitate the production of well-ordered crystals because they can provide additional protein contacts within the crystal and can preclude the protein–detergent micelle from participating in crystal contacts.

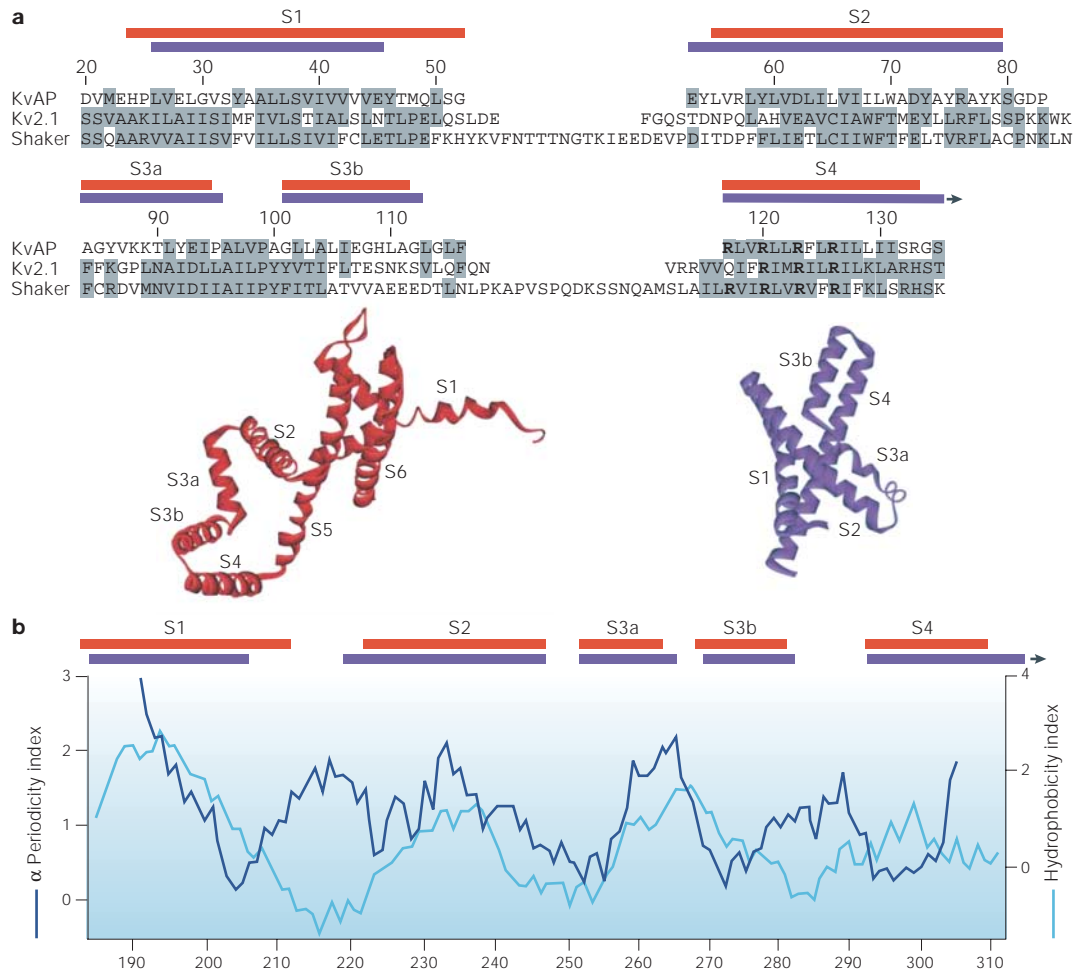


Figure 6 | **Sequence alignment for Kv channels and comparison of helical assignments.** **a** | Sequence alignments of Kv channels indicating the position of helices in the structures of the intact KvAP channel (red bars) and isolated S1–S4 domain (purple bars). Grey shading indicates similarity in sequence among the potassium channels. Basic residues in S4 are shown in bold text. **b** | Windowed α -periodicity index analysis from scanning mutagenesis of S1–S4 (REF. 99) using a sliding 13-residue window (dark blue line) superimposed with windowed hydrophobicity index analysis (light blue line)¹⁴³. There is good agreement between the helical assignments from mutagenesis (corresponding to peaks in the α -periodicity index) and the position of helices from the X-ray structures (red and purple bars).

SECONDARY STRUCTURE

The local conformation of the polypeptide backbone of a protein can adopt two types of secondary structure that are stabilized by regular hydrogen-bonding interactions between backbone carbonyl and amide groups. The most common secondary structure is the right-handed α -helix, which contains 3.6 residues per turn. The other secondary structure is the β -sheet, which is stabilized by hydrogen bonds between carbonyl and amide groups on two separate β -strands.

TERTIARY STRUCTURE

Tertiary structure refers to the higher order arrangement of secondary protein structures, including loops and linkers, to form the three dimensional structure of the protein.

Despite these discrepancies, MacKinnon and colleagues concluded that the crystallized full-length channel is not very far from a membrane-bound conformation²⁰. At present, the extent to which the structure of KvAP is distorted remains a central issue in the debate. The following are reasons to be concerned that the distortions are extensive.

Dearth of packing in the S1–S4 helices. There is a remarkable agreement between the secondary structure of S1–S4 from scanning mutagenesis studies in eukaryotic Kv channels^{43,99,115,116} and the KvAP X-ray structures (FIG. 6). The premise behind scanning approaches is that they can detect underlying helical periodicity if the presumptive helix resides in a bimodal environment, where one face of the helix tolerates substitution because it is exposed to solvent (either lipid or water) and the other does not because it is involved in packing with other parts of the protein^{118,119}. However, in the X-ray structure of KvAP, there is a marked absence of regular packing between the

5 helices in the S1–S4 domain, some of which are completely surrounded by lipids or water. This arrangement would not be expected to yield interpretable patterns in scanning mutagenesis studies, which indicates that either the agreement in the secondary structure is a coincidence, or that the tertiary structure and packing in the KvAP X-ray structure does not represent the membrane-embedded channel.

MTS accessibility of residues in the voltage-sensor. Studies of S4 in both a Nav channel and the Shaker Kv channel show that Cys introduced along the length of S4 can react with water soluble MTS reagents from one side of the membrane or the other^{46,47,89}. For the external end of S4, the rates of reaction for external MTS reagents differed by as little as 2-fold between resting and activated conformations of the voltage-sensor. The high degree of accessibility can be explained either by membrane-translocating movements of S4 or by crevices in the protein that provide a pathway for MTS reagents to access residues within

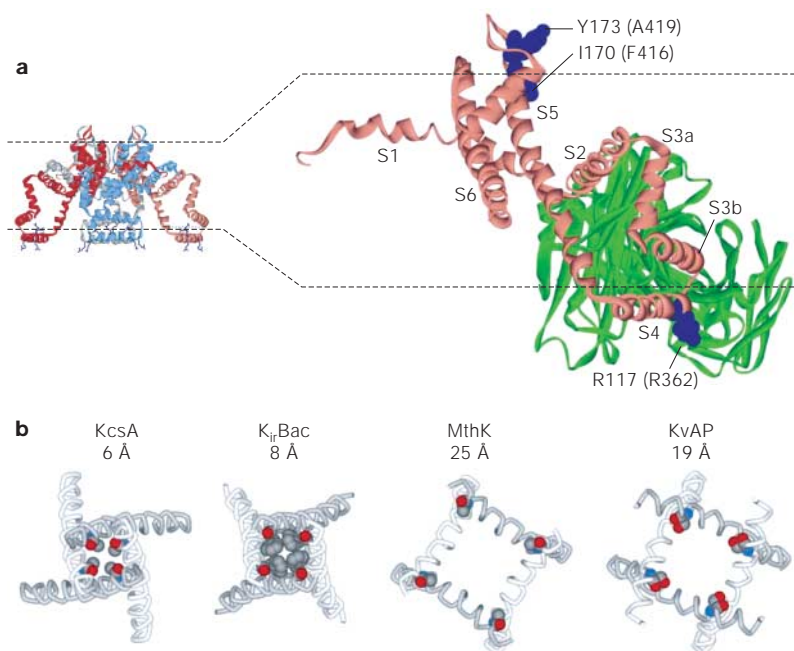


Figure 7 | X-ray structure of KvAP indicating the positions of important residues and a Fab fragment, and comparison of the intracellular pore aperture. **a** | X-ray structure of KvAP with a Fab fragment (green) and residues that are shown to crosslink in the Shaker Kv channel (dark blue). The residue number for KvAP is shown along with the numbering for Shaker in parentheses. The residues in S4 and S5 are shown in the same subunit, but the crosslinks and metal bridges are intersubunit¹⁰⁵, which places them further apart than is shown in the single subunit. **b** | The inner pore helices from the X-ray structures of four K⁺ channels, viewed from an intracellular vantage point. The distances given are between β -carbons on opposite subunits for equivalent residues in a narrow region of the gate (alanine 111 for KcsA, phenylalanine 146 in KvBac, lysine 95 in MthK and serine 232 in KvAP).

the membrane-spanning portion of the protein. However, the small differences in accessibility are difficult to reconcile with the KvAP structure and membrane translocation models, in which the resting S4 segment should be submerged in the membrane and inaccessible to extracellular MTS reagents. (The hydrophobic environment of the membrane should limit access of the hydrophilic MTS reagents, as well as suppress the formation of the thiolate anion that is the MTS-reactive species of the Cys sulphhydryl moiety^{120,121}) Furthermore, recent studies that investigated the reaction between MTS reagents and Cys residues introduced to the C terminus of S3 — which has been proposed to move as a unit with S4 (REF. 122) — show similar small changes in reaction rates for resting and activated states^{100,123,124}. These results indicate that the C-terminal end of S3 and the N-terminal end of S4 are positioned near the extracellular side of the membrane, both when the voltage-sensor is resting and activated.

Protein toxins binding to the voltage-sensor paddle. Hanatoxin, a protein toxin from tarantula venom, inhibits Kv channel gating when added to the extracellular solution¹¹³. Both scanning mutagenesis and gating current studies indicate that the toxin binds to the S3b helix in the voltage-sensor paddle motif^{42,43,114} and stabilizes a resting conformation of the voltage-sensors⁴⁴.

Although the toxin could reach into the membrane to interact with buried voltage-sensor paddles¹²⁵, its amphipathic character¹²⁶ makes it more likely that the interaction between the toxin and membrane occurs near the interface between polar head groups and hydrocarbon tails⁴⁴. As the interface between the toxin and the channel involves both strong hydrophobic and polar side chain interactions^{42,127}, the S3b helix is probably positioned close to the extracellular edge of the membrane when in a resting conformation. This idea is not consistent with the X-ray structure of KvAP.

Bridges between S4 and S5. Two pairs of residues in the Shaker Kv channel have been shown to form disulphide bonds and metal bridges between the N terminus of S4 and the C terminus of S5 (REF. 105). Intersubunit bridges between Cys or His residues that are substituted for the first arginine in S4 (362) and the alanine at 419 in S5 (FIG. 7) result in channels that are much more easily opened by membrane depolarization (that is, the P_o-V relation is shifted to negative voltages). In contrast, metal bridges between the same position in S4 and 416 in S5 (one helical turn below 419) result in channels that require stronger depolarization to open. Crosslinking between other pairs of residues between S4 and S5 has been inferred from functional studies^{107,108,128}. Interestingly, the affinity of metal bridges between 362 and 419 is quite high (~100 nM)¹⁰⁵, suggesting that these residues are in close proximity when the voltage-sensors are in both resting and activated conformations. Although metal bridges between 362 and 416 are weaker¹⁰⁵, the simplest interpretation of this bridge is that these residues are most optimally positioned for bridging when the voltage-sensor is in a resting conformation. Therefore, the bridges between 362 in S4 and both 416 and 419 in S5 indicate that these residues are not far apart in either resting or activated conformations of the voltage-sensor, which is difficult to reconcile with the X-ray structure of KvAP where the distance between these residues in adjacent subunits is between 60–80 Å.

Electron microscopy reconstruction of the KvAP channel. The structure of KvAP was recently analysed using electron microscopy and single particle reconstruction to produce a map of the protein with Fab fragments bound at 10.5 Å resolution¹²⁹. The conditions for these experiments are similar to those used to solve the X-ray structure of the channel, except that the protein solution is diluted to yield single particles. Earlier electrophysiological experiments show that the Fab fragments only bind to the paddle on the extracellular side of the membrane, and apparently require activation of the voltage-sensors¹²². In the electron microscopy maps of KvAP (at 0 mV), the Fab fragments are located on the extracellular side of the channel, indicating that the reconstruction represents the activated channel. The S6 gate is in the open conformation, which is also consistent with this hypothesis. Although the resolution of these maps is too low to reveal the position of individual side chains, there are two possible orientations of the paddle motif

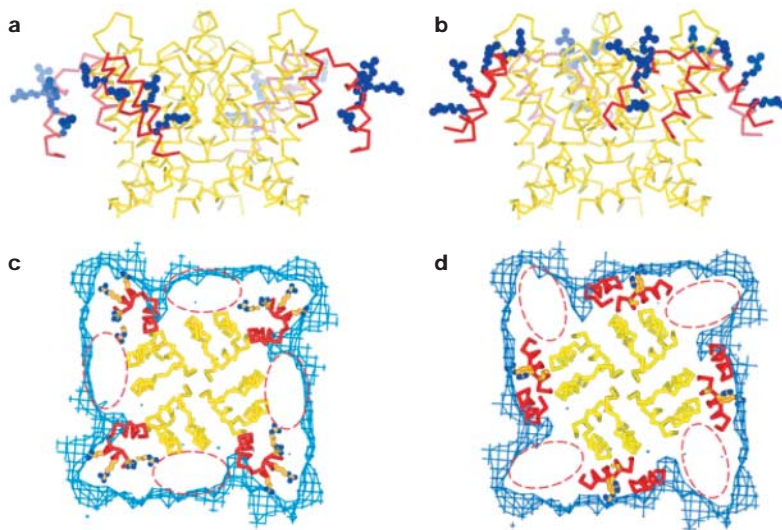


Figure 8 | Electron microscopy reconstruction of the KvAP channel with two possible orientations of the paddle relative to the pore. a, b | Two orientations of the paddle (red) are shown beside the pore (yellow). Arginine residues on S4 are shown in blue. **c, d** | Cross sections of the map (blue mesh) at the extracellular surface with the paddle and the pore in position. The extra density (highlighted by red dashed ovals) could be accounted for by S1, S2 and S3a for each possible orientation of the paddle. Reprinted, with permission, from REF. 129 © (2004) Macmillan Magazines Ltd.

(FIG. 8). In both cases, the S4 and S3b helices are positioned perpendicular to the membrane plane, with the tip of the paddle near the extracellular solution and the remaining helices in the voltage-sensing domain (S1, S2 and S3a) displaced to one side so that S4 would directly contact the lipid if the protein were in a native membrane (FIG. 8). This arrangement of the S1–S4 helices in the electron microscopy structure differs markedly when compared to the X-ray structures of KvAP and the isolated S1–S4 domain (FIG. 5).

The common thread running through most of the evidence for distortions in the X-ray structure of KvAP is that the N terminus of S4 and the S3b helix are probably positioned much closer to the extracellular edge of the membrane in both resting and activated conformations. The main source of distortion is likely to be the Fab fragment, which binds the paddle motif and is used to stabilize the protein for crystallization. The distorting influence of the Fab fragments might be related to their involvement in packing within the crystal, but may also involve a repositioning of the paddle that is intrinsic to the Fab–paddle interaction.

Evidence for the membrane translocation model
The original paddle model for gating charge movement is a membrane translocation model that is supported by an intuitive interpretation of how and why the KvAP structure is distorted, and by functional experiments^{20,122}. In this model, the distortion of KvAP is viewed as relatively minor, mainly arising from a paddle motif (S3b and S4) that is connected to the remaining protein through flexible S3 loops and S4–S5 linkers. The paddle position is distorted by crystal packing forces that are imposed by the Fab fragments bound to the tip of the

paddle. The helix–turn–helix paddle motif is intrinsically stable owing to tight packing at the helix–helix interface, but is flexible in its movement as a unit because of its flexible connections to the rest of the protein.

Guided by the apparent flexibility of the paddle, Jiang and colleagues¹²² asked whether the paddle translocates across the membrane by investigating whether AVIDIN (added to external or internal solutions) could bind to biotinylated residues in the paddle motif — an approach that has been used to study membrane translocating events associated with diphtheria toxins and colicins^{130–132}. The expected distance between the introduced Cys residues and the surface of avidin (with the biotin moiety bound inside) is about 10 Å. Biotin incorporated at thirteen positions in the paddle reacts with avidin from the extracellular side of the membrane but not the intracellular side (FIG. 9a,b red residues), and at two positions the reaction can be detected with intracellular but not extracellular avidin (FIG. 9a,b dark blue residues). Biotin attached at two other positions in S4 can react with avidin applied to either side (FIG. 9a,b yellow residues). This pattern of accessibility to avidin is consistent with a large membrane translocating event. The electron microscopy reconstruction is roughly consistent with the paddle model in that the paddle motif is located near the extracellular solution in the activated conformation and is extensively exposed to lipids. It will be interesting to address whether residues that are accessible to internal avidin at negative membrane voltages become inaccessible at depolarized voltages, and vice versa for external accessibility, by examining the state dependence for reactions between biotin and avidin. Although some qualitative experiments of this type have been reported¹²², a quantitative assessment of the state dependence could address whether avidin traps a rare conformation of the voltage-sensor. Furthermore, it will be important to test whether the interaction between S3b and S4 remains stable as the channel gates, which is an assumption in the interpretation of these experiments.

A controversial element of the paddle model is that charged residues in S4 might be able to traverse the hydrophobic phase of the membrane. (Note, however, that the interaction of basic residues with counter-charges in other parts of the protein is discussed¹²².) Although the presence of naked basic residues in the hydrophobic core of the membrane is energetically unfavorable (see below), the MscS channel^{133,134}, a prokaryotic stretch-activated cation channel, has two Arg residues that might be exposed to the hydrophobic phase of the membrane, so perhaps KvAP is not alone.

Evidence for the focused field model

Early evidence for the focused field model comes from studies of the reactivity between MTS reagents and Cys residues that are substituted in S4 (see above)^{45,46,87,100,123,124}. The hanatoxin⁴⁴ and bridging¹⁰⁵ experiments discussed above also support a focused field model to the extent that they point to an extracellular location of S3b and the N terminus of S4. Unlike the X-ray structure of KvAP, the electron microscopy reconstruction of KvAP¹²⁹ is compatible with the focused field model because the

AVIDIN

A 57 kDa tetrameric protein from egg white that binds the vitamin biotin with extremely high affinity ($K_d \sim 10^{-15}$ M). Biotin derivatives are available that can be tethered to proteins using various reactions, including maleimide chemistry for attachment to cysteine residues.

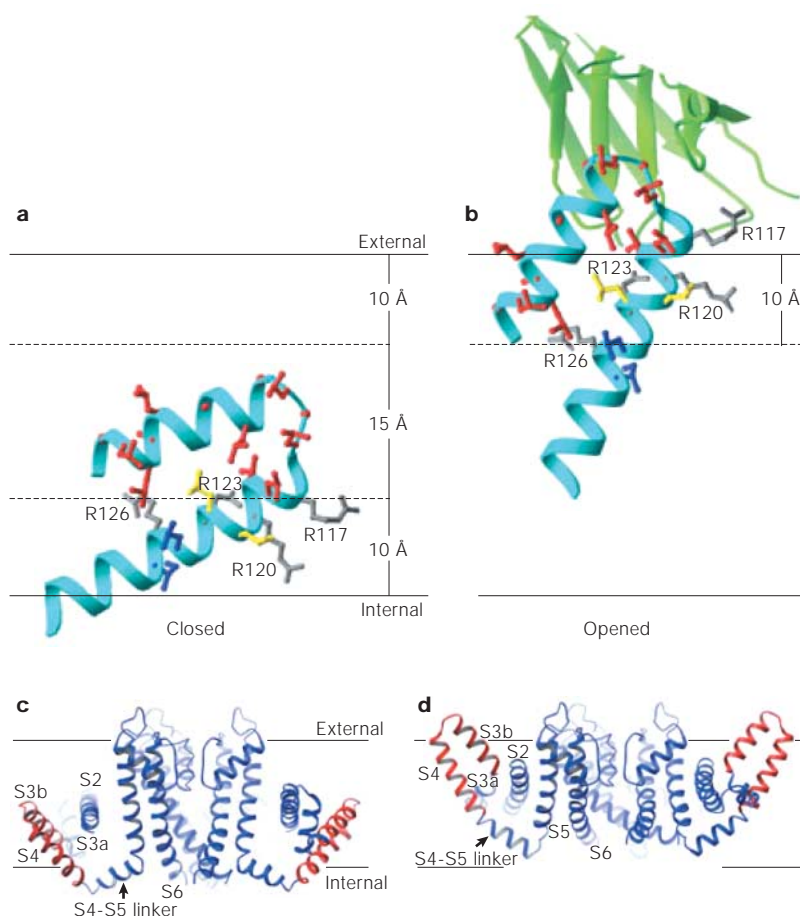


Figure 9 | A model showing the positions, in the membrane, of the voltage-sensor paddles during closed (resting) and opened (activated) conformations, and a hypothesis for coupling to pore opening. a, b | Closed (**a**) and opened (**b**) positions of the paddles derived from tethered biotin–avidin measurements, and structural and functional measurements with Fab fragments. A voltage-sensor paddle is shown as a cyan ribbon with red side chains indicating positions where attached biotin is accessible to external avidin, dark blue side chains where biotin is accessible to internal avidin, and yellow side chains where biotin is accessible to avidin on both sides of the membrane. Grey side chains show four arginine residues (R117, R120, R123 and R126) on the paddle, and the green ribbon in (**b**) shows part of a bound Fab fragment from the crystal structures. Solid horizontal lines show the external and internal membrane surfaces, and dashed lines indicate the 10-Å distance from the surfaces that are set by biotin and its linker. **c** | The closed KvAP structure is based on the paddle depth and orientation in **a** (red), and on adjusting the S5 and S6 helices of KvAP to the positions in KcsA, a K⁺ channel. **d** | The opened KvAP structure is based on the paddle depth and orientation in **b** (red), and the pore of KvAP. Reprinted, with permission, from REF 122 © (2003) Macmillan Magazines Ltd.

FLUORESCENCE RESONANCE ENERGY TRANSFER (FRET). The process by which an excited fluorophore (the donor) transfers energy to another molecule (the acceptor) when the emissions spectrum of the donor overlaps the absorption spectrum of the acceptor. The distance over which energy transfer is 50% efficient, the Förster distance, is typically in the range of 20–60 Å, making FRET useful as a spectroscopic ruler for distance measurements in proteins.

S3 and S4 segments have transmembrane orientations. The discussion below focuses on results that support the focused field model without specifically addressing the tertiary structure of the voltage-sensing domain.

In the focused field model, the charges in S4 do not interact with the hydrophobic phase of the membrane, but move between water-filled crevices and countercharges in S1–S3. The partitioning of amino-acid analogues between water and organic solvents indicate that moving basic residues (Arg and lysine) into the hydrophobic phase of the membrane is energetically costly¹³⁵. In principle, fluorescence experiments where fluorophores are attached to S4 can address whether S4 moves between aqueous and hydrophobic

environments because a shift in the emissions spectrum of the fluorophore should occur with partitioning between hydrophobic and aqueous environments¹³⁶. Interestingly, the emissions spectrum for tetramethylrhodamine maleimide (TMRM) is independent of whether the fluorophore is dissolved in water or attached to the N-terminal end of S4, but it undergoes a marked blue-shift when dissolved in hydrophobic solvents⁹¹, indicating that the N terminus of S4 is exposed to an aqueous environment. In addition, although the quantum yield for TMRM that is attached to S4 decreases in response to membrane depolarization (paralleling the Q–V relation), there is no shift in the emission spectra^{91,92}, a result that conflicts with the type of partitioning that is proposed in the paddle model.

The distance that charges need to move to cross the electric field is minimized in the focused field model. FLUORESCENCE RESONANCE ENERGY TRANSFER (FRET) has been used to estimate distances between donor and acceptor molecules attached to the end of the S4 segment in the Shaker Kv channel^{93,94,102,137}. The results indicate that S4 undergoes small movements (<5 Å) during activation, and are consistent with a rotation or tilting of the helix rather than a large transmembrane motion. Although these studies do not provide a consensus on the motion of S4, they agree on the small magnitude of movements — an observation that is easier to reconcile with the focused field model than with the membrane translocation model.

A remarkable phenomenon that has been observed in Kv channels is that the introduction of a His residue at the first Arg in the S4 segment of Shaker creates a proton conduction pathway when the voltage-sensor is in the resting conformation¹⁰¹. In the membrane translocation model, S4 should be completely buried in the membrane at rest, so invoking a coincidental and convoluted proton wire through the membrane-spanning portions of the protein would be required to explain this. In contrast, the small movements of charged residues between aqueous crevices in the focused field model could account for the shuttling of protons by an introduced His.

The notion that the first four Arg residues in S4 carry most of the gating charge in the Shaker Kv channel is based on experiments in which basic residues were neutralized and the effects on total charge per channel were assessed by measuring total gating charge and channel number^{75,76}. Ahern and Horn⁸⁸ carried out an elegant version of this experiment by introducing Cys residues, reacting them with charged MTS reagents and then assessing the effects of the added moiety on total charge per channel in the same cell. As well as confirming the importance of the first four Arg residues, they found that only the native Arg positions could carry charge. Adding charged adducts at positions that are neutral in the native channel (but interspersed between crucial Arg residues) does not increase the amount of charge that is moved when the channel is activated. This remarkable specificity is consistent with the focused field model but not the membrane translocation model.

Towards a structural model of voltage-sensing
 Although the membrane translocation and focused field models are useful for considering the mechanisms underlying voltage-sensing, neither model has a solid structural framework. As distorted as the KvAP X-ray structure might be, there is little evidence to support the type of shrouding of S4 by the S1–S3 segments that is indicated by many focused field models^{102–106,138}. The good news is that a consensus seems to be developing on several points, despite the uncertainties surrounding the structure of the voltage-sensor. For example, the close apposition of S4 and the pore domain (S5–S6) in the activated state is supported by distance measurements between sites labelled in the N terminus of S4 (REFS 93,94,139), the bridging between S4 and S5 (REFS 105,107,108), as well as the electron microscopy structure of KvAP (REF 129). In addition, perhaps the most consistent message from the X-ray and electron microscopy studies is that S4 would be significantly exposed to lipids if embedded in the membrane. This idea is supported by recent EPR experiments¹⁴⁰ that show extensive exposure of S4 to lipid soluble reagents. Although most residues in the S4 helix seem to be exposed to lipids in the EPR study, most of the charged Arg residues are not, indicating that they are protected from the membrane and interacting with other parts of the protein. The positioning of S4 at the lipid-protein interface might be easier to accept once it is divorced from any specific model of voltage-sensing. Indeed, the exposure of S4 to lipids is not inconsistent with the focused field model because the Arg residues in S4 could move through crevices between this segment and the remaining protein.

Although a consensus may be developing on certain aspects of voltage-sensor structure, the tertiary structure in this region is poorly constrained and many apparent contradictions remain to be resolved. The three structures of KvAP, for example, give different views on the structure of the voltage-sensor (FIGS 5,8). The EPR studies supporting lipid exposure of S4 also point to a lack of such exposure for S1 (REF 140), which stands in contrast to scanning mutagenesis studies on two eukaryotic Kv channels^{99,115} where a lipid-exposed face for S1 was consistently identified. This situation might be rectified by new structures of KvAP in defined conformations or of other 6 transmembrane segment ion channels (especially that of a prokaryotic Nav channel^{22,23}). It will also be important to carefully investigate the spatial proximity of specific residues within well defined secondary structural elements of the voltage-sensors. Our present understanding of bridges and crosslinks between S4 and S5 could be extended by examining the state-dependence of bridging, as has so elegantly been done in the gate region of the channel^{55,56,67}. It would also be advantageous to apply the various experimental approaches to the same protein. Indeed, most of the evidence for the membrane translocation model is from studies on KvAP, whereas that for the focused field model comes mainly from studies on Shaker. It really wouldn't be much fun if the present controversy were the result of diversity in the underlying structures and mechanisms, as seems to be the case for the gate region of the channel. The evidence to date for lipid exposure of S4 is interesting and should provoke new studies on the interaction between just about everything and membrane lipids¹⁴¹. This has not been a fashionable aspect of ion channel biology, but the provocative new structural models of Kv channels may soon change that.

1. Hodgkin, A. L. & Huxley, A. F. The components of membrane conductance in the giant axon of *Loligo*. *J. Physiol.* **116**, 473–496 (1952).
2. Hodgkin, A. L. & Huxley, A. F. Currents carried by sodium and potassium ions through the membrane of the giant axon of *Loligo*. *J. Physiol.* **116**, 449–472 (1952).
3. Hodgkin, A. L. & Huxley, A. F. The dual effect of membrane potential on sodium conductance in the giant axon of *Loligo*. *J. Physiol.* **116**, 497–506 (1952).
4. Hodgkin, A. L. & Huxley, A. F. A quantitative description of membrane current and its application to conduction and excitation in nerve. *J. Physiol.* **117**, 500–544 (1952).
5. Papazian, D. M., Schwarz, T. L., Tempel, B. L., Jan, Y. N. & Jan, L. Y. Cloning of genomic and complementary DNA from Shaker, a putative potassium channel gene from *Drosophila*. *Science* **237**, 749–753 (1987).
6. Timpe, L. C. *et al.* Expression of functional potassium channels from Shaker cDNA in *Xenopus* oocytes. *Nature* **331**, 143–145 (1988).
7. Zagotta, W. N., Hoshi, T. & Aldrich, R. W. Shaker potassium channel gating. III: Evaluation of kinetic models for activation. *J. Gen. Physiol.* **103**, 321–362 (1994).
8. Zagotta, W. N., Hoshi, T., Dittman, J. & Aldrich, R. W. Shaker potassium channel gating. II: Transitions in the activation pathway. *J. Gen. Physiol.* **103**, 279–319 (1994).
9. Hoshi, T., Zagotta, W. N. & Aldrich, R. W. Shaker potassium channel gating. I: Transitions near the open state. *J. Gen. Physiol.* **103**, 249–278 (1994).
10. Schoppa, N. E. & Sigworth, F. J. Activation of Shaker potassium channels. III. An activation gating model for wild-type and V2 mutant channels. *J. Gen. Physiol.* **111**, 313–342 (1998).
11. Schoppa, N. E. & Sigworth, F. J. Activation of Shaker potassium channels. II. Kinetics of the V2 mutant channel. *J. Gen. Physiol.* **111**, 295–311 (1998).
12. Schoppa, N. E. & Sigworth, F. J. Activation of Shaker potassium channels. I. Characterization of voltage-dependent transitions. *J. Gen. Physiol.* **111**, 271–294 (1998).
13. Islas, L. D. & Sigworth, F. J. Voltage sensitivity and gating charge in Shaker and Shab family potassium channels. *J. Gen. Physiol.* **114**, 723–741 (1999).
14. Soler-Llavina, G. J., Holmgren, M. & Swartz, K. J. Defining the conductance of the closed state in a voltage-gated K⁺ channel. *Neuron* **38**, 61–67 (2003).
15. Doyle, D. A. *et al.* The structure of the potassium channel: molecular basis of K⁺ conduction and selectivity. *Science* **280**, 69–77 (1998).
The first X-ray structure of a potassium channel. The KcsA potassium channel is a prokaryotic channel from *Streptomyces lividans* that was crystallized in a closed conformation.
16. Zhou, Y., Morais-Cabral, J. H., Kaufman, A. & MacKinnon, R. Chemistry of ion coordination and hydration revealed by a K⁺ channel–Fab complex at 2.0 Å resolution. *Nature* **414**, 43–48 (2001).
17. Zhou, M., Morais-Cabral, J. H., Mann, S. & MacKinnon, R. Potassium channel receptor site for the inactivation gate and quaternary amine inhibitors. *Nature* **411**, 657–661 (2001).
18. Jiang, Y. *et al.* Crystal structure and mechanism of a calcium-gated potassium channel. *Nature* **417**, 515–522 (2002).
The first X-ray structure of a potassium channel in the open conformation. This paper also shows the octameric arrangement of the RCK domains that form a gating ring on the intracellular side of the channel. A detailed discussion of gating motions is presented in the companion paper, reference 60.
19. Kuo, A. *et al.* Crystal structure of the potassium channel KirBac1.1 in the closed state. *Science* **300**, 1922–1926 (2003).
20. Jiang, Y. *et al.* X-ray structure of a voltage-dependent K⁺ channel. *Nature* **423**, 33–41 (2003).
21. Dutzler, R., Campbell, E. B., Cadene, M., Chait, B. T. & MacKinnon, R. X-ray structure of a CIC chloride channel at 3.0 Å reveals the molecular basis of anion selectivity. *Nature* **415**, 287–294 (2002).
22. Ren, D. *et al.* A prokaryotic voltage-gated sodium channel. *Science* **294**, 2372–2375 (2001).
23. Kolishi, R. *et al.* A superfamily of voltage-gated sodium channels in bacteria. *J. Biol. Chem.* **279**, 9532–9538 (2004).
24. Noda, M. *et al.* Expression of functional sodium channels from cloned cDNA. *Nature* **322**, 826–828 (1986).
25. Noda, M. *et al.* Existence of distinct sodium channel messenger RNAs in rat brain. *Nature* **320**, 188–192 (1986).
26. Tanabe, T. *et al.* Primary structure of the receptor for calcium channel blockers from skeletal muscle. *Nature* **328**, 313–318 (1987).
27. Goulding, E. H. *et al.* Molecular cloning and single-channel properties of the cyclic nucleotide-gated channel from catfish olfactory neurons. *Neuron* **8**, 45–58 (1992).
28. Santoro, B. *et al.* Identification of a gene encoding a hyperpolarization-activated pacemaker channel of brain. *Cell* **93**, 717–729 (1998).
29. Butler, A., Tsunoda, S., McCobb, D. P., Wei, A. & Salkoff, L. *mSlo*, a complex mouse gene encoding 'maxi' calcium-activated potassium channels. *Science* **261**, 221–224 (1993).
30. Kubo, Y., Reuveny, E., Slesinger, P. A., Jan, Y. N. & Jan, L. Y. Primary structure and functional expression of a rat G-protein-coupled muscarinic potassium channel. *Nature* **364**, 802–806 (1993).
31. Kubo, Y., Baldwin, T. J., Jan, Y. N. & Jan, L. Y. Primary structure and functional expression of a mouse inward rectifier potassium channel. *Nature* **362**, 127–133 (1993).

32. Ho, K. *et al.* Cloning and expression of an inwardly rectifying ATP-regulated potassium channel. *Nature* **362**, 31–38 (1993).
33. Ketchum, K. A., Joiner, W. J., Sellers, A. J., Kaczmarek, L. K. & Goldstein, S. A. A new family of outwardly rectifying potassium channel proteins with two pore domains in tandem. *Nature* **376**, 690–695 (1995).
34. Goldstein, S. A., Bockenhauer, D., O'Kelly, I. & Zilberberg, N. Potassium leak channels and the KCNK family of two-P-domain subunits. *Nature Rev. Neurosci.* **2**, 175–184 (2001).
35. Chen, G. Q., Cui, C., Mayer, M. L. & Gouaux, E. Functional characterization of a potassium-selective prokaryotic glutamate receptor. *Nature* **402**, 817–821 (1999).
36. MacKinnon, R. Determination of the subunit stoichiometry of a voltage-activated potassium channel. *Nature* **350**, 232–235 (1991).
37. Liman, E. R., Tytgat, J. & Hess, P. Subunit stoichiometry of a mammalian K⁺ channel determined by construction of multimeric cDNAs. *Neuron* **9**, 861–871 (1992).
38. Hoshi, T., Zagotta, W. N. & Aldrich, R. W. Biophysical and molecular mechanisms of Shaker potassium channel inactivation. *Science* **250**, 533–538 (1990).
39. Zagotta, W. N., Hoshi, T. & Aldrich, R. W. Restoration of inactivation in mutants of Shaker potassium channels by a peptide derived from ShB. *Science* **250**, 568–571 (1990).
40. Santacruz-Tolosa, L., Huang, Y., John, S. A. & Papazian, D. M. Glycosylation of Shaker potassium channel protein in insect cell culture and in *Xenopus* oocytes. *Biochemistry* **33**, 5607–5613 (1994).
41. Holmgren, M., Jurman, M. E. & Yellen, G. N-type inactivation and the S4-S5 region of the Shaker K⁺ channel. *J. Gen. Physiol.* **108**, 195–206 (1996).
42. Li-Smerin, Y. & Swartz, K. J. Localization and molecular determinants of the hanatoxin receptors on the voltage-sensing domain of a K⁺ channel. *J. Gen. Physiol.* **115**, 673–684 (2000).
43. Li-Smerin, Y. & Swartz, K. J. Helical structure of the COOH terminus of S3 and its contribution to the gating modifier toxin receptor in voltage-gated ion channels. *J. Gen. Physiol.* **117**, 205–218 (2001).
44. Lee, H. C., Wang, J. M. & Swartz, K. J. Interaction between extracellular Hanatoxin and the resting conformation of the voltage-sensor paddle in K_v channels. *Neuron* **40**, 527–536 (2003).
- This paper investigates the effects of a protein toxin from tarantula venom on gating charge movement, which provides evidence for a relatively extracellular position for the S3b helix when the voltage sensors are in their resting conformations.**
45. Yang, N., George, A. L., Jr & Horn, R. Molecular basis of charge movement in voltage-gated sodium channels. *Neuron* **16**, 113–122 (1996).
46. Larsson, H. P., Baker, O. S., Dhillon, D. S. & Isacoff, E. Y. Transmembrane movement of the Shaker K⁺ channel S4. *Neuron* **16**, 387–397 (1996).
47. Yusaf, S. P., Wray, D. & Sivaprasadarao, A. Measurement of the movement of the S4 segment during the activation of a voltage-gated potassium channel. *Pflügers Arch.* **433**, 91–97 (1996).
48. MacKinnon, R. & Miller, C. Mechanism of charybdotoxin block of the high-conductance, Ca²⁺-activated K⁺ channel. *J. Gen. Physiol.* **91**, 335–349 (1988).
49. MacKinnon, R., Heginbotham, L. & Abramson, T. Mapping the receptor site for charybdotoxin, a pore-blocking potassium channel inhibitor. *Neuron* **5**, 767–771 (1990).
50. Armstrong, C. M. Inactivation of the potassium conductance and related phenomena caused by quaternary ammonium ion injection in squid axons. *J. Gen. Physiol.* **54**, 553–575 (1969).
51. Armstrong, C. M. Interaction of tetraethylammonium ion derivatives with the potassium channels of giant axons. *J. Gen. Physiol.* **58**, 413–437 (1971).
52. Armstrong, C. M. Ionic pores, gates, and gating currents. *Q. Rev. Biophys.* **7**, 179–210 (1974).
- An intelligent review that lays out a conceptual framework for understanding the mechanisms that underlie voltage-dependent gating and cation selectivity. This review was years ahead of its time and is a true classic in the field.**
53. Holmgren, M., Smith, P. L. & Yellen, G. Trapping of organic blockers by closing of voltage-dependent K⁺ channels: evidence for a trap door mechanism of activation gating. *J. Gen. Physiol.* **109**, 527–535 (1997).
- This paper clearly shows the trapping of quaternary ammonium compounds in the intracellular pore of the Shaker potassium channel.**
54. Liu, Y., Holmgren, M., Jurman, M. E. & Yellen, G. Gated access to the pore of a voltage-dependent K⁺ channel. *Neuron* **19**, 175–184 (1997).
- A classic paper that shows the gated access of MTS reagents for Cys residues substituted in the intracellular region of the S6 segment in the Shaker potassium channel.**
55. del Camino, D. & Yellen, G. Tight steric closure at the intracellular activation gate of a voltage-gated K⁺ channel. *Neuron* **32**, 649–656 (2001).
56. Holmgren, M., Shin, K. S. & Yellen, G. The activation gate of a voltage-gated K⁺ channel can be trapped in the open state by an intrasubunit metal bridge. *Neuron* **21**, 617–621 (1998).
57. Sukhareva, M., Hackos, D. H. & Swartz, K. J. Constitutive activation of the Shaker K_v channel. *J. Gen. Physiol.* **122**, 541–556 (2003).
58. Kitaguchi, T., Sukhareva, M. & Swartz, K. J. Stabilizing the closed S6 gate in the Shaker K_v channel through modification of a hydrophobic seal. *J. Gen. Physiol.* **124**, 319–332 (2004).
59. Roux, B., Berneche, S. & Im, W. Ion channels, permeation, and electrostatics: insight into the function of KcsA. *Biochemistry* **39**, 13295–13306 (2000).
60. Jiang, Y. *et al.* The open pore conformation of potassium channels. *Nature* **417**, 523–526 (2002).
61. Perozo, E., Cortes, D. M. & Cuello, L. G. Structural rearrangements underlying K⁺-channel activation gating. *Science* **285**, 73–78 (1999).
62. Liu, Y. S., Sompornpisut, P. & Perozo, E. Structure of the KcsA channel intracellular gate in the open state. *Nature Struct. Biol.* **8**, 883–887 (2001).
63. Kelly, B. L. & Gross, A. Potassium channel gating observed with site-directed mass tagging. *Nature Struct. Biol.* **10**, 280–284 (2003).
64. Irizarry, S. N., Kutluay, E., Drews, G., Hart, S. J. & Heginbotham, L. Opening the KcsA K⁺ channel: tryptophan scanning and complementation analysis lead to mutants with altered gating. *Biochemistry* **41**, 13653–13662 (2002).
65. MacArthur, M. W. & Thornton, J. M. Influence of proline residues on protein conformation. *J. Mol. Biol.* **218**, 397–412 (1991).
66. Del Camino, D., Holmgren, M., Liu, Y. & Yellen, G. Blocker protection in the pore of a voltage-gated K⁺ channel and its structural implications. *Nature* **403**, 321–325 (2000).
67. Webster, S. M., Del Camino, D., Dekker, J. P. & Yellen, G. Intracellular gate opening in Shaker K⁺ channels defined by high-affinity metal bridges. *Nature* **428**, 864–868 (2004).
- This paper investigates metal bridges in the gate region of the Shaker potassium channel that are not compatible with the X-ray structures of either KcsA, which was crystallized in a closed conformation, or MthK, which was crystallized in an open conformation.**
68. Armstrong, C. M. & Bezanilla, F. Currents related to movement of the gating particles of the sodium channels. *Nature* **242**, 459–461 (1973).
69. Armstrong, C. M. & Bezanilla, F. Charge movement associated with the opening and closing of the activation gates of the Na channels. *J. Gen. Physiol.* **63**, 533–552 (1974).
70. Keynes, R. D. & Rojas, E. Kinetics and steady-state properties of the charged system controlling sodium conductance in the squid giant axon. *J. Physiol.* **239**, 393–434 (1974).
71. Schneider, M. F. & Chandler, W. K. Voltage dependent charge movement of skeletal muscle: a possible step in excitation-contraction coupling. *Nature* **242**, 244–246 (1973).
72. Chandler, W. K., Schneider, M. F., Rakowski, R. F. & Adrian, R. H. Charge movements in skeletal muscle. *Phil. Trans. R. Soc. Lond. B* **270**, 501–505 (1975).
73. Bezanilla, F. & Stefani, E. Gating currents. *Methods Enzymol.* **293**, 331–352 (1998).
74. Schoppa, N. E., McCormack, K., Tanouye, M. A. & Sigworth, F. J. The size of gating charge in wild-type and mutant Shaker potassium channels. *Science* **255**, 1712–1715 (1992).
75. Aggarwal, S. K. & MacKinnon, R. Contribution of the S4 segment to gating charge in the Shaker K⁺ channel. *Neuron* **16**, 1169–1177 (1996).
76. Seoh, S. A., Sigg, D., Papazian, D. M. & Bezanilla, F. Voltage-sensing residues in the S2 and S4 segments of the Shaker K⁺ channel. *Neuron* **16**, 1159–1167 (1996).
77. Nocell, F. *et al.* Effective gating charges per channel in voltage-dependent K⁺ and Ca²⁺ channels. *J. Gen. Physiol.* **108**, 143–155 (1996).
78. Hirschberg, B., Rovner, A., Lieberman, M. & Patlak, J. Transfer of twelve charges is needed to open skeletal muscle Na⁺ channels. *J. Gen. Physiol.* **106**, 1053–1068 (1995).
79. Auld, V. J. *et al.* A neutral amino acid change in segment IIIS4 dramatically alters the gating properties of the voltage-dependent sodium channel. *Proc. Natl Acad. Sci. USA* **87**, 323–327 (1990).
80. Papazian, D. M., Timpe, L. C., Jan, Y. N. & Jan, L. Y. Alteration of voltage-dependence of Shaker potassium channel by mutations in the S4 sequence. *Nature* **349**, 305–310 (1991).
81. Liman, E. R., Hess, P., Weaver, F. & Koren, G. Voltage-sensing residues in the S4 region of a mammalian K⁺ channel. *Nature* **353**, 752–756 (1991).
82. Smith-Maxwell, C. J., Ledwell, J. L. & Aldrich, R. W. Uncharged S4 residues and cooperativity in voltage-dependent potassium channel activation. *J. Gen. Physiol.* **111**, 421–439 (1998).
83. Smith-Maxwell, C. J., Ledwell, J. L. & Aldrich, R. W. Role of the S4 in cooperativity of voltage-dependent potassium channel activation. *J. Gen. Physiol.* **111**, 399–420 (1998).
84. Ledwell, J. L. & Aldrich, R. W. Mutations in the S4 region isolate the final voltage-dependent cooperative step in potassium channel activation. *J. Gen. Physiol.* **113**, 389–414 (1999).
85. Perozo, E., Santacruz-Tolosa, L., Stefani, E., Bezanilla, F. & Papazian, D. M. S4 mutations alter gating currents of Shaker K channels. *Biophys. J.* **66**, 345–354 (1994).
86. Ahern, C. A. & Horn, R. Specificity of charge-carrying residues in the voltage sensor of potassium channels. *J. Gen. Physiol.* **123**, 205–216 (2004).
- A recent paper that examines where in S4 the addition of charged MTS moieties contributes to the total gating charge per channel. The results indicate that only the positions that are charged in the wild-type channel are capable of contributing to gating charge.**
87. Yang, N. & Horn, R. Evidence for voltage-dependent S4 movement in sodium channels. *Neuron* **15**, 213–218 (1995).
- A classic study that investigated the movements of S4 by measuring the voltage-dependence of the reaction between MTS reagents and Cys residues substituted in S4.**
88. Starace, D. M., Stefani, E. & Bezanilla, F. Voltage-dependent proton transport by the voltage sensor of the Shaker K⁺ channel. *Neuron* **19**, 1319–1327 (1997).
89. Starace, D. M. & Bezanilla, F. Histidine scanning mutagenesis of basic residues of the S4 segment of the Shaker K⁺ channel. *J. Gen. Physiol.* **117**, 469–490 (2001).
90. Mannuzzu, L. M., Moronne, M. M. & Isacoff, E. Y. Direct physical measure of conformational rearrangement underlying potassium channel gating. *Science* **271**, 213–216 (1996).
- This was the first study that investigated S4 movements using fluorescence spectroscopy.**
91. Cha, A. & Bezanilla, F. Characterizing voltage-dependent conformational changes in the Shaker K⁺ channel with fluorescence. *Neuron* **19**, 1127–1140 (1997).
92. Cha, A. & Bezanilla, F. Structural implications of fluorescence quenching in the Shaker K⁺ channel. *J. Gen. Physiol.* **112**, 391–408 (1998).
93. Glauner, K. S., Mannuzzu, L. M., Gandhi, C. S. & Isacoff, E. Y. Spectroscopic mapping of voltage sensor movement in the Shaker potassium channel. *Nature* **402**, 813–817 (1999).
94. Cha, A., Snyder, G. E., Selvin, P. R. & Bezanilla, F. Atomic scale movement of the voltage-sensing region in a potassium channel measured via spectroscopy. *Nature* **402**, 809–813 (1999).
95. Gandhi, C. S., Loots, E. & Isacoff, E. Y. Reconstructing voltage sensor-pore interaction from a fluorescence scan of a voltage-gated K⁺ channel. *Neuron* **27**, 585–595 (2000).
96. Papazian, D. M. *et al.* Electrostatic interactions of S4 voltage sensor in Shaker K⁺ channel. *Neuron* **14**, 1293–1301 (1995).
97. Planells-Cases, R., Ferrer-Montiel, A. V., Patten, C. D. & Montal, M. Mutation of conserved negatively charged residues in the S2 and S3 transmembrane segments of a mammalian K⁺ channel selectively modulates channel gating. *Proc. Natl Acad. Sci. USA* **92**, 9422–9426 (1995).
98. Tiwari-Woodruff, S. K., Schulteiss, C. T., Mock, A. F. & Papazian, D. M. Electrostatic interactions between transmembrane segments mediate folding of Shaker K⁺ channel subunits. *Biophys. J.* **72**, 1489–1500 (1997).
99. Li-Smerin, Y., Hackos, D. H. & Swartz, K. J. Alpha-helical structural elements within the voltage-sensing domains of a K⁺ channel. *J. Gen. Physiol.* **115**, 33–50 (2000).
100. Nguyen, T. P. & Horn, R. Movement and crevices around a sodium channel S3 segment. *J. Gen. Physiol.* **120**, 419–436 (2002).
101. Starace, D. M. & Bezanilla, F. A proton pore in a potassium channel voltage sensor reveals a focused electric field. *Nature* **427**, 548–553 (2004).
- This paper shows the creation of a proton-conducting pore within the voltage-sensor of the Shaker potassium channel.**
102. Bezanilla, F. Voltage sensor movements. *J. Gen. Physiol.* **120**, 465–473 (2002).
- An excellent review of what is known about how S4 moves during gating in voltage-activated channels.**

103. Horn, R. Coupled movements in voltage-gated ion channels. *J. Gen. Physiol.* **120**, 449–453 (2002).
104. Gandhi, C. S. & Isacoff, E. Y. Molecular models of voltage sensing. *J. Gen. Physiol.* **120**, 455–463 (2002).
105. Laine, M. *et al.* Atomic proximity between S4 segment and pore domain in Shaker potassium channels. *Neuron* **39**, 467–481 (2003).
- A rigorous demonstration of disulphide and metal bridge formation between residues in the N terminus of S4 and the C terminus of S5.**
106. Laine, M., Papazian, D. M. & Roux, B. Critical assessment of a proposed model of Shaker. *FEBS Lett.* **564**, 257–263 (2004).
107. Gandhi, C. S., Clark, E., Loots, E., Pralle, A. & Isacoff, E. Y. The orientation and molecular movement of a K⁺ channel voltage-sensing domain. *Neuron* **40**, 515–525 (2003).
108. Broomand, A., Mannikko, R., Larsson, H. P. & Elinder, F. Molecular movement of the voltage sensor in a K⁺ channel. *J. Gen. Physiol.* **122**, 741–748 (2003).
109. Ahern, C. A. & Horn, R. Stirring up controversy with a voltage sensor paddle. *Trends Neurosci.* **27**, 303–307 (2004).
110. Cohen, B. E., Grabe, M. & Jan, L. Y. Answers and questions from the KvAP structures. *Neuron* **39**, 395–400 (2003).
111. Ruta, V., Jiang, Y., Lee, A., Chen, J. & MacKinnon, R. Functional analysis of an archaeobacterial voltage-dependent K⁺ channel. *Nature* **422**, 180–185 (2003).
112. Miller, C. The charybdotoxin family of K⁺ channel-blocking peptides. *Neuron* **15**, 5–10 (1995).
113. Swartz, K. J. & MacKinnon, R. Hanatoxin modifies the gating of a voltage-dependent K⁺ channel through multiple binding sites. *Neuron* **18**, 665–673 (1997).
114. Swartz, K. J. & MacKinnon, R. Mapping the receptor site for hanatoxin, a gating modifier of voltage-dependent K⁺ channels. *Neuron* **18**, 675–682 (1997).
115. Hong, K. H. & Miller, C. The lipid-protein interface of a Shaker K⁺ channel. *J. Gen. Physiol.* **115**, 51–58 (2000).
116. Monks, S. A., Needleman, D. J. & Miller, C. Helical structure and packing orientation of the S2 segment in the Shaker K⁺ channel. *J. Gen. Physiol.* **113**, 415–423 (1999).
117. Tu, L., Wang, J., Helm, A., Skach, W. R. & Deutsch, C. Transmembrane biogenesis of Kv1.3. *Biochemistry* **39**, 824–836 (2000).
118. Comette, J. L. *et al.* Hydrophobicity scales and computational techniques for detecting amphipathic structures in proteins. *J. Mol. Biol.* **195**, 659–685 (1987).
119. Rees, D. C., DeAntonio, L. & Eisenberg, D. Hydrophobic organization of membrane proteins. *Science* **245**, 510–513 (1989).
120. Li, J., Shi, L. & Karlin, A. A photochemical approach to the lipid accessibility of engineered cysteinyl residues. *Proc. Natl Acad. Sci. USA* **100**, 886–891 (2003).
121. Karlin, A. & Akabas, M. H. Substituted-cysteine accessibility method. *Methods Enzymol.* **293**, 123–145 (1998).
122. Jiang, Y., Ruta, V., Chen, J., Lee, A. & MacKinnon, R. The principle of gating charge movement in a voltage-dependent K⁺ channel. *Nature* **423**, 42–48 (2003).
- This study probes the movement of the voltage-sensor paddle motif in KvAP by biotinylating specific sites and assaying for reaction with avidin, added to either external or internal solutions. The authors propose a new paddle model for voltage-sensing in which the paddle motif undergoes a relatively large membrane translocating movement during gating.**
123. Blaustein, R. O. Kinetics of tethering quaternary ammonium compounds to K⁺ channels. *J. Gen. Physiol.* **120**, 203–216 (2002).
124. Carter, A., Ketty, V. & Blaustein, R. O. State-dependent reactivity of cysteines substituted into Shaker's gating module. *Biophys. J.* **86**, 192 (2004).
125. Lee, S. Y. & MacKinnon, R. A membrane-access mechanism of ion channel inhibition by voltage sensor toxins from spider venom. *Nature* **430**, 232–235 (2004).
126. Takahashi, H. *et al.* Solution structure of hanatoxin1, a gating modifier of voltage-dependent K⁺ channels: common surface features of gating modifier toxins. *J. Mol. Biol.* **297**, 771–780 (2000).
127. Wang, J. M. *et al.* Molecular surface of tarantula toxins interacting with voltage sensors in K_v channels. *J. Gen. Physiol.* **123**, 455–467 (2004).
128. Neale, E. J., Elliott, D. J., Hunter, M. & Sivaprasadarao, A. Evidence for intersubunit interactions between S4 and S5 transmembrane segments of the Shaker potassium channel. *J. Biol. Chem.* **278**, 29079–29085 (2003).
129. Jiang, Q. X., Wang, D. N. & MacKinnon, R. Electron microscopic analysis of K_vAP voltage-dependent K⁺ channels in an open conformation. *Nature* **430**, 806–810 (2004).
130. Senzel, L., Huynh, P. D., Jakes, K. S., Collier, R. J. & Finkelstein, A. The diphtheria toxin channel-forming T domain translocates its own NH2-terminal region across planar bilayers. *J. Gen. Physiol.* **112**, 317–324 (1998).
131. Slatin, S. L., Qiu, X. Q., Jakes, K. S. & Finkelstein, A. Identification of a translocated protein segment in a voltage-dependent channel. *Nature* **371**, 158–161 (1994).
132. Oh, K. J., Senzel, L., Collier, R. J. & Finkelstein, A. Translocation of the catalytic domain of diphtheria toxin across planar phospholipid bilayers by its own T domain. *Proc. Natl Acad. Sci. USA* **96**, 8467–8470 (1999).
133. Bass, R. B. *et al.* The structures of BtuCD and MscS and their implications for transporter and channel function. *FEBS Lett.* **555**, 111–115 (2003).
134. Bass, R. B., Strop, P., Barclay, M. & Rees, D. C. Crystal structure of *Escherichia coli* MscS, a voltage-modulated and mechanosensitive channel. *Science* **298**, 1582–1587 (2002).
135. Fersht, A. *Structure and Mechanism in Protein Science: a Guide to Enzyme Catalysis and Protein Folding* 336–337 (W. H. Freeman, New York, 1999).
136. Lakowicz, J. R. *Principles of Fluorescence Spectroscopy* (Kluwer Academic/Plenum, New York, 1999).
137. Blunck, R., Starace, D. M., Correa, A. M. & Bezanilla, F. Detecting rearrangements of Shaker and NaChBac in real-time with fluorescence spectroscopy in patch-clamped mammalian cells. *Biophys. J.* **86**, 3966–3980 (2004).
138. Durell, S. R., Hao, Y. & Guy, H. R. Structural models of the transmembrane region of voltage-gated and other K⁺ channels in open, closed, and inactivated conformations. *J. Struct. Biol.* **121**, 263–284 (1998).
139. Blaustein, R. O., Cole, P. A., Williams, C. & Miller, C. Tethered blockers as molecular 'tape measures' for a voltage-gated K⁺ channel. *Nature Struct. Biol.* **7**, 309–311 (2000).
140. Cuello, L., Cortes, D. M. & Perozo, E. Molecular architecture of the K_vAP voltage-dependent K⁺ channel in a lipid bilayer. *Science* **306**, 491–495 (2004).
- A timely EPR study investigating the mobility and environmental exposure (water vs lipid) of spin labels attached to specific positions throughout S1–S4.**
141. Gutberlet, T. & Katsaras, J. *Lipid Bilayers: Structure and Interactions* (Springer, Berlin; New York, 2001).
142. Perozo, E., MacKinnon, R., Bezanilla, F. & Stefani, E. Gating currents from a nonconducting mutant reveal open-closed conformations in Shaker K⁺ channels. *Neuron* **11**, 353–358 (1993).
143. Kyte, J. & Doolittle, R. F. A simple method for displaying the hydrophobic character of a protein. *J. Mol. Biol.* **157**, 105–132 (1982).

Acknowledgements
I thank M. Holmgren, Z. Lu, J. Mindell, E. Perozo, S. Silberberg and the members of the Swartz laboratory for helpful discussions.

Competing interests statement
The author declares no competing financial interests.

 **Online links**

FURTHER INFORMATION
Encyclopedia of Life Sciences: <http://www.els.net/>
Calcium channels | Ion channels | Membrane potential | Sodium, calcium and potassium channels | Voltage-gated potassium channels
Swartz's laboratory:
http://neuroscience.nih.gov/Lab.asp?Org_ID=55
Access to this interactive links box is free online.